Site-Selective Functionalization of Molecularly Imprinted Nanoparticles to Recognize Lysine-Rich Peptides

Avijit Ghosh and Yan Zhao*

Department of Chemistry, Iowa State University, Ames, Iowa 50011-3111, U.S.A.

ABSTRACT: Sequence-selective binding of peptides is a long-standing goal of chemists. As one of the most abundant amino acids in proteins, lysine plays important roles in protein functions, as well as in antimicrobial and cell-penetrating peptides. Herein, we report molecularly imprinted nanoparticles with high sequence selectivity for lysine-rich peptides. The nanoparticles are prepared from molecular imprinting of cross-linkable surfactant micelles and postmodification of the imprinted pockets by photoaffinity labeling. The method allows carboxylic acids to be installed precisely near the lysine amino side chains, greatly enhancing the binding strengths for lysine-rich peptides. Small variations of the peptide sequence can be distinguished and the binding affinity correlates positively with the number of lysine groups in model tripeptides. The method applies to complex lysine-rich biological peptides, achieving hundreds of nanomolar of binding affinities and excellent binding specificities.

INTRODUCTION

Sequence-selective recognition of peptides has been a long-standing goal in bioorganic and supramolecular chemistry, due to the importance of peptides and proteins in biology. Chemists have used various platforms over the years to bind peptides, including molecular tweezers and clips, cucurbiturils, sequences, gold nanoparticles (NPs), and co-assembled amphiphiles. Although it is now possible to target certain side chains of amino acids and some short sequences using carefully designed supramolecular hosts, most synthetic peptide receptors cannot recognize a long strand of peptide with sequence selectivity.

From the supramolecular chemistry point of view, the challenge in sequence-selective binding of peptides is enormous, even if the peptide only contains a few amino acid residues. With 20 different building blocks, a pentapeptide has 3.2 million possible combinations. To differentiate these sequences, a combination of hydrophobic and polar interactions have to be used, demanding a rather complex receptor in terms of binding functionalities and structural scaffolding. Some amino acids differ minutely in their structures; extreme precision is thus required for the molecular recognition.

As the most abundant amino acid on the surface of both cytoplasmic and extracellular proteins, lysine plays an important role in the stability of proteins and their nonspecific interactions. ¹² It is one of the most post-translationally modified residues, undergoing acetylation, methylation, ubiquitination, glutarylation, and many others. ^{13,14} These modifications regulate a myriad of biological functions including chromatin structure, enzyme activities, protein–protein interactions, and cellular location. Lysine-rich peptides also play certain unique roles in biology. Among them are antimicrobial peptides ^{15,16} and cell-penetrating peptides ¹⁷⁻²¹ that utilize the cationic charges of the side chains to bind negative groups on cell

membranes, to destabilize membrane or to migrate across them, respectively.

Our group has reported molecularly imprinted nanoparticles (MINPs) with strong abilities to recognize peptides.²² Functional monomers (FMs)²³ or cross-linkers²⁴ can be introduced to enhance the binding of basic peptides. However, these strategies require the peptide templates to be incorporated into micelles efficiently for effective molecular imprinting and are thus challenging for totally hydrophilic peptides.

In this work, we report a method to molecularly imprintly sinerich peptides even if the peptides do not possess any hydrophobic residues. Carboxylic acid binding groups are installed inside the MINP pockets, precisely matching the lysine residues of the peptide templates. Large enhancement in the binding affinity is achieved, and the protein-sized water-soluble nanoparticle receptors display excellent sequence selectivity in both model tripeptides and longer biological peptides. Molecular imprinting is a powerful method to create polymeric receptors for biological molecules and peptidebinding materials have been reported.²⁵⁻³³ The lysine-binding MINPs in this work serve as the bridge between molecularly based supramolecular peptide binders and much larger nanoparticles or macroscopic molecularly imprinted peptide-binding materials. Their comparable size (~5 nm) to many proteins makes them potentially useful to probe protein functions or intervene in biological processes.

EXPERIMENTAL SECTION

General Procedure for the MINP Preparation (Scheme 1). 34 To a micellar solution of compound 2 (8.4 mg, 0.02 mmol) in H_2O (2.0 mL), divinylbenzene (DVB, 0.02 mmol), 1 in DMSO (0.0008 mmol), and 2,2-dimethoxy-2-phenylacetophenone

(DMPA, 10 µL of a 12.8 mg/mL solution in DMSO, 0.0005 mmol) were added. The mixture was subjected to ultrasonication for 20 min. Then the peptide template (0.0004 mmol) was added and stirred at 60 rpm for 12 h. Then diazide cross-linker 3 (4.13 mg, 0.024 mmol), CuCl₂ (10 μ L of a 6.7 mg/mL solution in H₂O, 0.0005 mmol), and sodium ascorbate (10 μL of a 99 mg/mL solution in H₂O, 0.005 mmol) were added. After the reaction mixture was stirred slowly (at 60 rpm) at room temperature for 12 h, mono azide 4 (15 mg, 0.06 mmol), CuCl₂ (10 µL of a 6.7 mg/mL solution in H_2O , 0.0005 mmol 1), and sodium ascorbate (10 μ L of a 99 mg/mL solution in H₂O, 0.005 mmol) were added. After being stirred (at 90 rpm) for another 6 h at room temperature, the reaction mixture was transferred to a glass vial, purged with nitrogen for 15 min, sealed with a rubber stopper, and irradiated in a Rayonet reactor for 6 h. The reaction mixture was poured into acetone (8 mL). The precipitate was collected by centrifugation (2500 × g for 10 min) and washed with a mixture of acetone/water (5 mL/1 mL) three times. The crude produce was washed thrice with methanol/acetic acid (5 mL/0.1 mL). The off-white/yellow powder was dried in the air to afford the final MINPs with a typical yield of 70–80%.

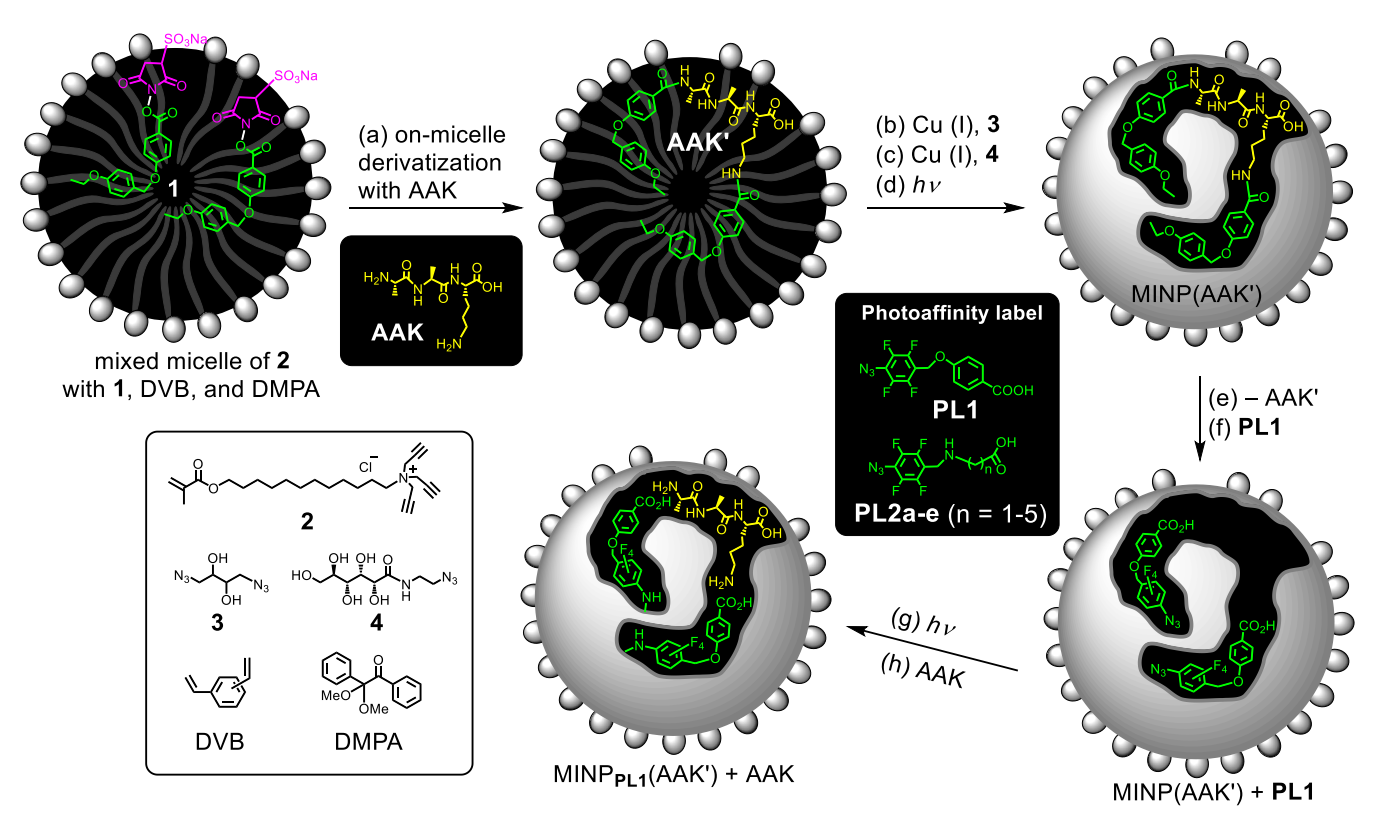
General Procedure for the Photoaffinity Labeling of MINP (Scheme 1). A 10.0 mg (0.0002 mmol) portion of the MINP was dissolved in 1.0 mL of water, followed by the addition of the photoaffinity label PL1 or PL2a–e (0.0002 mmol, 5 μ L from a stock solution in DMSO). The mixture was irradiated in a Rayonet reactor for 2 h before it was poured into acetone (40 mL). The precipitate collected by centrifugation (2500 \times g for 10 min) was washed with a mixture of acetone/water (5 mL/1 mL) three times, methanol/acetic acid (5 mL/0.1 mL) three times, and acetone twice (5 mL) before it was dried in air to afford the final photo labelled MINP

(typical yield 70–80%).

Determination of Binding Constants by ITC. In general, a solution of an appropriate guest oligopeptide in 10 mM (HEPES) buffer (pH 7.5) at 298 K was injected in equal steps into 1.43 mL of the corresponding MINPs in the same solution. An average molecular weight of 50 kDa was used for making the stock solutions of MINPs. The top panel shows the raw calorimetric data. The area under each peak represents the amount of heat generated at each ejection and is plotted against the molar ratio of the MINPs to the guest oligopeptides. The solid line is the best fit of the experimental data to the sequential binding of N equal and independent binding sites on the MINP. The heat of dilution for the substrate, obtained by adding the substrate to the buffer, was subtracted from the heat released during the binding. Binding parameters were autogenerated after curve fitting using Microcal Origin 7.

RESULTS AND DISCUSSION

Scheme 1 shows our method to create imprinted nanoparticles for AAK (i.e., alanine–alanine–lysine), our first lysine-containing model tripeptide. The key design is in the amphiphilic activated ester derivative 1. The anionic sulfo-succinimide derivative gets easily included into the cationic micelle of surfactant 1 via combined hydrophobic and electrostatic interactions. The sulfonate group anchors the molecules at the surfactant/water interface and helps them react in situ with a peptide added to the solution (step a). Most peptides are amphiphilic in nature and prefer to residue near the micelle surface. The higher local concentrations of the two are expected to facilitate the acylation of the peptide by 1, affording modified tripeptide AAK' solubilized in the micelle.



Scheme 1. Preparation of MINP_{PLI}(AAK') for selective binding of tripeptide AAK. The surface ligands (clicked 3) are omitted for clarity.

The micelle of **2** has a dense layer of terminal alkynes on the surface due to the tripropargylammonium headgroup of the surfactant. Diazide **3** in the presence of Cu(I) catalysts readily cross-links the micelle surface by the highly efficient alkyne–azide cycloaddition (step b). The click reaction is used again (step c) to decorate the micelle with multiple copies of monoazide **4** (omitted from the drawings in Scheme 1 for clarity). With divinylbenzene (DVB) and 2,2-dimethoxy-2-phenyl-acetophenone (DMPA, a photoinitiator) solubilized in the interior, the micelle is then cross-linked in the core by UV-induced free radical polymerization (step d).

The resulting MINP(AAK'), i.e., MINP prepared with AAK' as the template, is purified by precipitation into acetone and solvent washing to remove the template. Photoaffinity label (PL) **PL1** is subsequently added to the redissolved MINP(AAK') in water. The size and shape of the green-colored substructure of AAK' is designed purposefully to resemble **PL1**, meaning that the PL has a strong hydrophobic driving force to enter the imprinted pockets formerly occupied by the (green-colored) hydrophobic side chains of AAK'.

Phenyl azides are well-established photoaffinity labels³⁵ and those containing ortho fluoro groups are known to undergo C–H insertion efficiently under UV irradiation through an aromatic nitrene intermediate.³⁶ A hydrophobic microenvironment promotes singlet nitrene formation, which is especially suited for C–H insertion.^{37,38} Once the nitrene is generated inside a pocket within MINP(AAK'), it can react with a nearby C–H bond to covalently install a carboxylic acid to the imprinted pocket. The resulting MINP_{PL1}(AAK') has two carboxylic acids positioned precisely to match the two amino groups of the template, one near the N-terminus and the other close to the lysine side chain.

There are multiple reasons to perform the in situ peptide derivatization of the peptide in the micelle prior to the imprinting. First, as described above, it enables our "bait-and-switch" strategy to swap the "hydrophobic anchors" of the derivatized AAK' with the covalently installed carboxylic acid binding groups. Second, AAK' has a higher propensity to enter micelles than the less hydrophobic parent AAK. A higher imprinting efficiency is expected as a result of better template incorporation into the micelle. Third, the amphiphilicity of AAK' suggests that the peptide portion of the template will be located near the surface of the micelle (to be properly solvated by water molecules), while the hydrophobic anchors are deeper in the hydrophobic micelle core. Such a topology is expected to be helpful to both the template removal and rebinding of AAK afterwards.

Table 1 shows the binding properties of MINP_{PLI}(AAK'), i.e., MINP prepared with AAK' as the template and postfunctionalized with **PL1**. Without the peptide derivatization and photoaffinity-based postfunctionalization, AAK also undergoes micellar imprinting, but the binding is about half of that using 1 equivalent of the sulfo-succinimide modifier (1) in the imprinting procedure (compare entries 1 and 2). After photoaffinity labeling of the imprinted pockets, the binding constant increases further, with a nearly 4-fold increase (compare entries 1 and 3).

AAK has two amino groups. Consistent with our design, two equivalents of the sulfo-succinimide modifier (1) bring an even larger increase in the binding constant, for both the as-prepared MINP(AAK') and the post-functionalized MINP_{PLI}(AAK') (Table 1, entries 4–5). Further increases in the amounts of the modifier bring no additional benefits (entries 6–9), suggesting that the in situ derivatization is highly efficient. We have optimized the time

required for the derivatization to occur (Table S1). Under our experimental conditions (0.2 mM of peptide, 0.4 mM of 1, and 10 mM of surfactant in water at room temperature), the reaction takes about 12 h to go to completion, before the micellar imprinting is performed directly without separation of the derivatized peptide.

Table 1. Binding properties of MINP_{PL}(AAK') determined by isothermal titration calorimetry (ITC).^a

| entry | [AAK]/[1] | PL | $K_{\rm a}$ | -Δ <i>G</i> | |
|-------|-----------|------|------------------------|-------------|--|
| | | rL | $(\times 10^4 M^{-1})$ | (kcal/mol) | |
| 1 | 1:0 | none | 17.6 ± 0.8 | 7.16 | |
| 2 | 1:1 | none | 32.1 ± 5.9 | 7.51 | |
| 3 | 1:1 | PL1 | 65.4 ± 6.2 | 7.93 | |
| 4 | 1:2 | none | 51.9 ± 5.7 | 7.80 | |
| 5 | 1:2 | PL1 | 114.0 ± 27.4 | 8.26 | |
| 6 | 1:3 | none | 57.2 ± 6.6 | 7.85 | |
| 7 | 1:3 | PL1 | 106.0 ± 14.9 | 8.22 | |
| 8 | 1:4 | none | 47.1 ± 2.1 | 7.74 | |
| 9 | 1:4 | PL1 | 77.8 ± 9.3 | 8.04 | |
| 10 | 1:2 | PL2a | 85.3 ± 11.8 | 8.09 | |
| 11 | 1:2 | PL2b | 129.0 ± 23.5 | 8.34 | |
| 12 | 1:2 | PL2c | 156.0 ± 30.5 | 8.45 | |
| 13 | 1:2 | PL2d | 137.0 ± 15.8 | 8.37 | |
| 14 | 1:2 | PL2e | 102.0 ± 15.6 | 8.20 | |

^a Titrations were performed at 298 K in 10mM HEPES buffer (pH=7.5) in triplicates, with the errors between runs <10%.

The data so far indicate that the in situ derivatization of the peptide AAK is highly efficient, requiring only 1 equivalent of the modifier per amino group even at a low concentration (0.2 mM). Photoaffinity labeling is also very helpful, boosting the binding constant by more than 6 times even though the peptide only contains one lysine (compare entries 1 and 5).

PL1 was initially chosen for its close resemblance to the (greencolored) hydrophobic anchor of AAK'. A few other PLs (**PL2a-e**, Scheme 1) were also tested. Instead of a more rigid benzoic acid moiety, these molecules have a linear amino acid attached to the fluorinated phenyl azide. The hypothesis is that the skinner and more flexible tether might allow the carboxyl binding groups to adjust their positions and orientations to better interact with the lysine-containing peptides.

Consistent with our design, the resulting MINP_{PL2a-e}(AAK') nanoparticles bind AAK with a tether-dependent fashion and the binding constant peaks at n = 3 for **PL2c**, although one more or less methylene group in the tether also gives strong binding (Table 1, entries 10-14).

We then used the optimized **PL2c** to make nanoparticle receptors for AKK and KKK, two tripeptides containing 2 and 3 lysines, respectively. Figure 1a shows the comparison of the binding properties of the photoaffinity-labelled receptors with those of the directly imprinted receptors as a function of the number of lysine residues. According to the ITC binding data, MINP_{PL2c}(AAK'), MINP_{PL2c}(AKK'), and MINP_{PL2c}(KKK') display a distinctive increase of binding with an increasing number of lysines in the template. In contrast, MINP(AAK), MINP(AKK), and MINP(KKK), the MINPs obtained from direct imprinting without any peptide derivatization and photoaffinity labeling, afford binding constants

about an order of magnitude lower. Not only so, a negative correlation between the binding constants and the number of lysines is observed (Figure 1a, red line) instead of the positive correlation (Figure 1a, black line). When the ratios of the binding constants between the photoaffinity labeled MINPs and the nonlabelled MINPs are plotted, Figure 1b shows that the photoaffinity labeling consistently boosts the binding. The enhancement factor (i.e., K_{+PL2c}/K_{-PL2c} in Figure 1b) increases almost linearly with the number of lysines in the peptide, ranging from 9 all the way to 30.

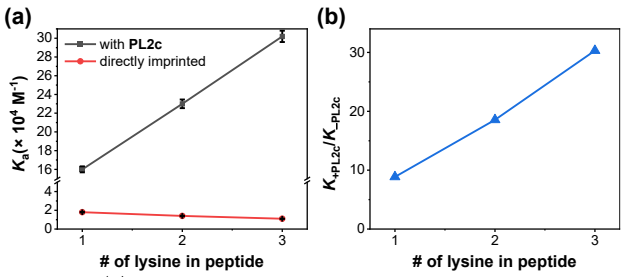


Figure 1. (a) Comparison of the binding properties of the photoaffinity-labelled MINPs with those of the directly imprinted MINPs as a function of the number of lysine residues. (b) Effects of photoaffinity labeling on the binding constant of MINPs as a function of the number of lysine residues.

The above results strongly support our overall design. Essentially, without the in situ peptide derivatization, a higher number of lysine makes the templating template more hydrophilic and more difficult to enter the micelles for imprinting (and also more difficult

to be bound afterwards due to their stronger solvation in water). The peptide derivatives from the sulfo-succinimide modifier (1), on the other hand, are highly hydrophobic and stay in micelles much better for more efficient imprinting. The carboxyl binding groups installed through the photoaffinity labeling later on also can form specific salt bridges/hydrogen bonds with the amino groups of the peptides. Both factors should contribute to the enhanced binding.

It is encouraging that the photoaffinity labeling greatly strengthens the binding for lysine-rich peptides. Another important parameter to consider is binding selectivity. After all, in a practical application, a peptide binder often has to differentiate other peptide sequences present, sometimes with small differences in the structure.

To understand the effects of the photoaffinity labelling on binding selectivities, we measured the binding constants of two differently labeled MINPs with the directly imprinted MINP(AAK) for a number of tripeptide analogues (Table 2). The peptide analogues have identical first and second amino acid residues (AA) and only differ in the last residue. A quick glance at the data reveals that all three MINPs have reasonable binding selectivities. Even through the photoaffinity labelled receptors have much stronger binding for AAK (compare entries 1, 7, and 13), there is no deterioration in the binding selectivity, evident from the relatively small $K_{\rm rel}$ values for the nontemplating peptides. In this work, $K_{\rm rel}$ is defined as the binding constant of an MINP receptor for a guest template relative to that of the templating peptide. The smaller the value, the higher is the binding selectivity.

Table 2. ITC binding data for different MINPs prepared for AAK.^a

| entry | MINP | guest | [AAK]/[1] | $K_{\rm a}$ | $K_{ m rel}$ | -ΔG | -ΔΗ | ΤΔS |
|-------|---------------------|-------|-----------|---------------------------------|--------------|------------|------------------|------------|
| Circi | | | | $(\times 10^4 \mathrm{M}^{-1})$ | 140 | (kcal/mol) | (kcal/mol) | (kcal/mol) |
| 1 | $MINP_{PL1}(AAK')$ | AAK | 1:2 | 114.0 ± 27.4 | 1 | 8.26 | 81.31 ± 4.16 | -73.05 |
| 2 | $MINP_{PL1}(AAK')$ | AAR | 1:2 | 35.3 ± 1.6 | 0.31 | 7.57 | 8.77 ± 0.01 | -1.20 |
| 3 | $MINP_{PL1}(AAK')$ | AAH | 1:2 | 33.8 ± 2.5 | 0.30 | 7.54 | 5.31 ± 0.11 | 2.23 |
| 4 | $MINP_{PL1}(AAK')$ | AAF | 1:2 | 21.8 ± 1.9 | 0.19 | 7.28 | 3.30 ± 0.10 | 3.98 |
| 5 | $MINP_{PL1}(AAK')$ | AAE | 1:2 | 25.2 ± 1.3 | 0.22 | 7.37 | 2.24 ± 0.04 | 5.13 |
| 6 | $MINP_{PL1}(AAK')$ | AAS | 1:2 | 34.1 ± 1.5 | 0.30 | 7.55 | 8.57 ± 0.10 | -1.02 |
| 7 | $MINP_{PL2c}(AAK')$ | AAK | 1:2 | 156.0 ± 30.5 | 1 | 8.45 | 24.56 ± 0.81 | -16.11 |
| 8 | $MINP_{PL2c}(AAK')$ | AAR | 1:2 | 38.2 ± 3.5 | 0.24 | 7.62 | 21.21 ± 0.67 | -13.59 |
| 9 | $MINP_{PL2c}(AAK')$ | AAH | 1:2 | 33.8 ± 3.3 | 0.22 | 7.54 | 35.09 ± 1.18 | -27.55 |
| 10 | $MINP_{PL2c}(AAK')$ | AAF | 1:2 | 23.6 ± 2.4 | 0.15 | 7.33 | 24.31 ± 0.73 | -16.98 |
| 11 | $MINP_{PL2c}(AAK')$ | AAE | 1:2 | 25.8 ± 1.3 | 0.17 | 7.38 | 7.62 ± 0.12 | -0.24 |
| 12 | $MINP_{PL2c}(AAK')$ | AAS | 1:2 | 36.7 ± 5.9 | 0.24 | 7.59 | 8.18 ± 0.40 | -0.59 |
| 13 | MINP(AAK) | AAK | 1:0 | 17.6 ± 0.8 | 1 | 7.16 | 3.55 ± 0.05 | 3.61 |
| 14 | MINP(AAK) | AAR | 1:0 | 6.10 ± 0.9 | 0.35 | 6.53 | 6.85 ± 0.44 | -0.32 |
| 15 | MINP(AAK) | AAH | 1:0 | 4.85 ± 0.7 | 0.28 | 6.39 | 6.62 ± 0.56 | -0.23 |
| 16 | MINP(AAK) | AAF | 1:0 | 2.15 ± 0.2 | 0.12 | 5.91 | 5.15 ± 0.70 | 0.76 |
| 17 | MINP(AAK) | AAE | 1:0 | 4.02 ± 1.8 | 0.23 | 6.28 | 4.10 ± 0.13 | 2.18 |
| 18 | MINP(AAK) | AAS | 1:0 | 5.51 ± 1.3 | 0.31 | 6.47 | 4.63 ± 0.68 | 1.84 |

^aTitrations were performed at 298 K in 10mM HEPES buffer (pH=7.5) in triplicates, with the errors between runs <10%.

Table 3. ITC binding data for different MINPs prepared for AKK.^a

| entry | host | guest | [AKK]/[1] | $K_{\rm a}$ (× 10 ⁴ M ⁻¹) | $K_{ m rel}$ | $-\Delta G$ (kcal/mol) | -ΔH (kcal/mol) | TΔS (kcal/mol) |
|-------|-----------------------------|-------|-----------|--|--------------|------------------------|-------------------|----------------|
| 1 | MINP _{PL2c} (AKK') | AKK | 1:3 | 232.0 ± 49.5 | 1 | 8.68 | 33.05 ± 0.77 | -24.37 |
| 2 | $MINP_{PL2c}(AKK')$ | ASK | 1:3 | 102.0 ± 9.4 | 0.44 | 8.20 | 77.41 ± 1.49 | -69.21 |
| 3 | $MINP_{PL2c}(AKK')$ | SSK | 1:3 | 59.8 ± 6.2 | 0.26 | 7.88 | 29.54 ± 0.72 | -21.66 |
| 4 | $MINP_{PL2c}(AKK')$ | KKK | 1:3 | 61.7 ± 6.8 | 0.27 | 7.90 | 29.60 ± 0.80 | -21.70 |
| 5 | $MINP_{PL2c}(AKK')$ | AKA | 1:3 | 67.7 ± 8.0 | 0.29 | 7.95 | 30.29 ± 0.81 | -22.34 |
| 6 | $MINP_{PL2c}(AKK')$ | KAA | 1:3 | 34.8 ± 1.6 | 0.15 | 7.56 | 36.81 ± 0.50 | -29.25 |
| 7 | $MINP_{PL2c}(AKK')$ | AAK | 1:3 | 96.4 ± 6.5 | 0.42 | 8.16 | 82.74 ± 1.10 | -74.58 |
| 8 | MINP(AKK) | AKK | 1:0 | 12.5 ± 0.8 | 1 | 6.95 | 10.03 ± 0.27 | -3.08 |
| 9 | MINP(AKK) | ASK | 1:0 | 6.11 ± 1.9 | 0.49 | 6.53 | 6.44 ± 1.10 | -0.09 |
| 10 | MINP(AKK) | SSK | 1:0 | 4.86 ± 0.7 | 0.39 | 6.39 | 2.74 ± 0.16 | 3.65 |
| 11 | MINP(AKK) | KKK | 1:0 | 2.99 ± 0.4 | 0.24 | 6.11 | 4.97 ± 0.65 | 1.14 |
| 12 | MINP(AKK) | AKA | 1:0 | 3.18 ± 0.7 | 0.25 | 6.14 | 9.78 ± 2.63 | -3.64 |
| 13 | MINP(AKK) | KAA | 1:0 | 2.69 ± 0.7 | 0.22 | 6.04 | 4.92 ± 1.24 | 1.12 |
| 14 | MINP(AKK) | AAK | 1:0 | 5.44 ± 0.5 | 0.44 | 6.46 | 8.96 ± 0.85 | -2.50 |

^aTitrations were performed at 298 K in 10 mM HEPES buffer (pH=7.5) in duplicates, with the errors between runs <10%.

The tripeptide tested include AAR and AAH, two peptides that also contain a basic residue at the third position. It is good that MINP_{PL1}(AAK') binds these two with only ~30% of the binding constant ($K_{\rm rel}$) in comparison to that of the templating peptide (Table 2, entries 1–3). Thus, even the very similar arginine (R) can be distinguished. Replacing the lysine with a hydrophobic residue (F), an acidic residue (E), or a neutral hydrophilic residue (S) all lowers the binding constant by 3–5-fold (entries 4–6), indicating that MINP_{PL1}(AAK') is strongly selective for its peptide target.

Our initial expectation is that **PL1**, which has a higher resemblance to the sulfo-succinimide modifier (1), might have better binding selectivities than **PL2c** which affords the strongest binding in Table 1. Instead, the $K_{\rm rel}$ values for MINP_{PL2c}(AAK') are consistently lower than those for MINP_{PL1}(AAK') (compare entries 8–12 with 2–6 in Table 2). Thus, the skinner and more flexible tethers in the carboxylic acid binding groups are helpful to both binding

affinity and specificity.

We then determined the binding constants of MINPs prepared with AKK and KKK as the templates and examined the effects of the photoaffinity labeling on the selectivities (Tables 3 and 4). For AKK, some of the peptide guests have a single residue variation (ASK, KKK, and AAK) and others have the positions of two residues switched (e.g., AKA). The general conclusion is that the photoaffinity labeling strongly enhances the binding strength (Table 3, entries 1 and 8) while maintaining the binding selectivities (compare entries 2–7 and 9–14). Similar results are obtained for KKK in Table 4.

Having confirmed the benefits of the photoaffinity labeling for lysine-rich peptides with the model compounds, we turned our attention to biological sequences found in natural proteins that contain 1–7 lysine residues (Figure 2). To our delight, the photoaffinity-labeled MINPs prepared using **PL2C** consistently outperform those made through direct imprinting, by more than 10-fold. For these

Table 4. ITC binding data for different MINPs prepared for KKK..a

| entry | host | guest | [KKK]/[1] | $K_{\rm a}$ | $K_{ m rel}$ | - ΔG | - ΔH | $T\Delta S$ |
|-------|---------------------|-------|--------------------|------------------------|--------------|--------------|------------------|-------------|
| entry | 11081 | guest | | $(\times 10^4 M^{-1})$ | Trei | (kcal/mol) | (kcal/mol) | (kcal/mol) |
| 1 | $MINP_{PL2c}(KKK')$ | KKK | 1:4 | 297.0 ± 86.2 | 1 | 8.83 | 62.55 ± 3.28 | -53.72 |
| 2 | $MINP_{PL2c}(KKK')$ | ASK | 1:4 | 62.1 ± 9.4 | 0.21 | 7.90 | 44.93 ± 0.04 | -16.11 |
| 3 | $MINP_{PL2c}(KKK')$ | SSK | 1:4 | 66.6 ± 1.2 | 0.22 | 7.94 | 32.38 ± 0.01 | -13.58 |
| 4 | $MINP_{PL2c}(KKK')$ | AKK | 1:4 | 97.6 ± 16 | 0.33 | 7.52 | 43.28 ± 0.09 | -27.46 |
| 5 | $MINP_{PL2c}(KKK')$ | AKA | 1:4 | 32.3 ± 1.4 | 0.11 | 7.52 | 34.71 ± 0.03 | -27.46 |
| 6 | $MINP_{PL2c}(KKK')$ | KAA | 1:4 | 60.5 ± 6.0 | 0.20 | 7.89 | 94.13 ± 0.01 | -0.16 |
| 7 | $MINP_{PL2c}(KKK')$ | AAK | 1:4 | 64.0 ± 5.4 | 0.22 | 7.92 | 97.7 ± 0.03 | -0.51 |
| 8 | MINP(KKK) | KKK | 1:0 | 9.8 ± 5.4 | 1 | 6.81 | 9.8 ± 0.03 | -2.99 |
| 9 | MINP(KKK) | ASK | 1:0 | 2.18 ± 0.5 | 0.22 | 5.92 | 5.5 ± 0.01 | -0.42 |
| 10 | MINP(KKK) | SSK | 1:0 | 2.86 ± 0.8 | 0.29 | 6.08 | 4.2 ± 0.01 | -1.88 |
| 11 | MINP(KKK) | AKK | 1:0 | 3.11 ± 0.4 | 0.32 | 6.13 | 9.0 ± 0.04 | -2.87 |
| 12 | MINP(KKK) | AKA | 1:0 | 2.69 ± 0.9 | 0.27 | 6.04 | 7.5 ± 0.09 | -1.46 |
| 13 | MINP(KKK) | KAA | 1:0 | 2.22 ± 0.9 | 0.23 | 5.93 | 3.7 ± 0.01 | -2.23 |
| 14 | MINP(KKK) | AAK | 1:0 | 2.65 ± 0.7 | 0.27 | 6.03 | 7.8 ± 0.09 | -1.77 |

^aTitrations were performed at 298 K in 10 mM HEPES buffer (pH=7.5) in duplicates, with the errors between runs <10%.

Table 5. ITC binding data for different MINPs prepared for PKKKRKV.^a

| | L | | [T]/[1] | $K_{\rm a}$ | | -∆G | -ΔΗ | $T\Delta S$ |
|-------|---------------------------------|-----------------------|----------|------------------------|--------------|------------|------------------|-------------|
| entry | host | guest | | $(\times 10^4 M^{-1})$ | $K_{ m rel}$ | (kcal/mol) | (kcal/mol) | (kcal/mol) |
| 1 | MINP _{PL2c} (PKKKRKV') | PKKKRKV | 1:5 | 605.0 ± 192 | 1 | 9.25 | 79.03 ± 0.03 | -69.78 |
| 2 | $MINP_{PL2c}(PKKKRKV')$ | KVFGRCE ^b | 1:5 | 1.90 ± 1.2 | 0.0031 | 5.84 | 3.83 ± 1.34 | 2.01 |
| 3 | $MINP_{PL2c}(PKKKRKV')$ | WDAYKNL | 1:5 | 2.02 ± 0.97 | 0.0033 | 5.87 | 2.02 ± 0.04 | 3.85 |
| 4 | MINP _{PL2c} (PKKKRKV') | VKFGVGEK | 1:5 | 3.02 ± 3.0 | 0.0050 | 6.11 | 7.12 ± 0.04 | -1.01 |
| 5 | MINP _{Pl2c} (PKKKRKV') | FRKKWNKWALSR | 1:5 | 4.21 ± 0.93 | 0.0070 | 6.31 | 5.20± 1.19 | 1.11 |
| 6 | MINP _{Pl2c} (PKKKRKV') | $YKQRVKNK^b$ | 1:5 | 4.0 ± 2.6 | 0.0066 | 6.28 | 2.13 ± 1.12 | 4.15 |
| 7 | MINP(PKKKRKV) | PKKKRKV | 1:0 | 35.8 ± 1.12 | 1 | 7.58 | 4.94 ± 0.03 | 2.64 |
| 8 | MINP(PKKKRKV) | KVFGRCE ^b | 1:0 | 3.57 ± 0.46 | 0.10 | 6.21 | 1.50 ± 0.11 | 4.71 |
| 9 | MINP(PKKKRKV) | WDAYKNL | 1:0 | 1.59 ± 0.60 | 0.044 | 5.73 | 1.78 ± 0.04 | 3.95 |
| 10 | MINP(PKKKRKV) | VKFGVGEK | 1:0 | 0.88 ± 0.28 | 0.025 | 5.38 | 0.78 ± 0.12 | 4.60 |
| 11 | MINP(PKKKRKV) | FRKKWNKWALSR | 1:0 | 0.61 ± 0.18 | 0.017 | 5.16 | 3.21 ± 1.73 | 1.95 |
| 12 | MINP(PKKKRKV) | YKQRVKNK ^b | 1:0 | 1.31 ± 0.73 | 0.037 | 5.62 | 0.99 ± 0.58 | 4.93 |
| a | | 200 II : 10 3 (LIEDE | c 1 cc / | TT = 5\ : 1 | 4. | 11 | 1 | 100/ h FEI |

^a Titrations were performed at 298 K in 10 mM HEPES buffer (pH=7.5) in duplicates, with the errors between runs <10%. ^b The C-terminal carboxyl is terminated with NH₂.

long biological peptides, hydrophobic residues are known to contribute significantly to the binding.²² Thus, even shorter sequences such as WDAYKNL and KVFGRCE easily display dissociation constants <400 nM, because they contain hydrophobic amino acids such as tryptophan (W), leucine (L), valine (V), and phenylalanine (F).

The biological peptides studied have more than one point of difference in the sequences (Figure 2). Thus, when the binding selectivities are studied, both the photoaffinity labeled and unlabeled MINPs display great specificity, with the non-templating peptides showing minimal bindings (Table 5).

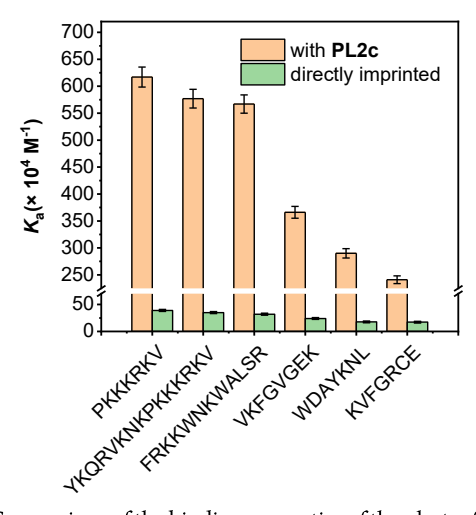


Figure 2. Comparison of the binding properties of the photoaffinity-labelled MINPs for lysine-containing biological peptides with those of the directly imprinted MINPs.

CONCLUSIONS

The small sizes (~ 5 nm) of MINPs make them particularly useful in applications that demand high precision at nanoscales such as inhibition of protein–protein interactions and mechanistic study of protein functions.^{39,40} Hydrophilic peptides are generally more difficult to imprint in cross-linked micelles because of their lower tendency to enter micelles.²² This work illustrates a strategy to imprint lysine-rich peptides even if they are completely hydrophilic, through

an in situ micelle-promoted chemical derivatization and facile photoaffinity labeling afterwards to install carboxyl groups precisely near the amino side chains of lysines. For KKK, our method affords a water-soluble polymeric nanoparticle receptor with $\sim\!340$ nM dissociation constant (Table 4, entry 1) or $\sim\!30$ -fold tighter binding in comparison to the nanoparticle receptor prepared through direct imprinting (Table 4, entries 8). What is important about the labeling is that binding selectivities are maintained (Tables 3 and 4) and sometimes improved (Tables 2 and 5) while the bindings for the targeted peptides are greatly strengthened. The method applies to small tripeptides and biological peptides with up to 15 amino acid residues. Thus, a general method for lysine-rich peptides is available for this important class of molecules, facilitating their biological studies.

ASSOCIATED CONTENT

Supporting Information

Synthetic procedures, characterization of compounds and materials, ITC binding curves, additional tables and figures, and NMR data. This material is available free of charge via the Internet at http://pubs.acs.org.

AUTHOR INFORMATION

Corresponding Author

Yan Zhao – Department of Chemistry, Iowa State University, Ames, Iowa 50011-3111, U.S.A.; E-mail: zhaoy@iastate.edu

Authors

Avijit Ghosh – Department of Chemistry, Iowa State University, Ames, Iowa 50011-3111, U.S.A.

ORCID

Avijit Ghosh: 0000-0002-8974-9565 Yan Zhao: 0000-0003-1215-2565

ACKNOWLEDGMENT

We thank NSF (DMR-2308625) for supporting the research.

REFERENCES

(1) Peczuh, M. W.; Hamilton, A. D. Peptide and Protein Recognition by Designed Molecules. *Chem. Rev.* **2000**, *100*, 2479-2494.

- (2) Maity, D.; Schmuck, C. In Synthetic Receptors for Biomolecules: Design Principles and Applications; The Royal Society of Chemistry, 2015; pp 326-368.
- (3) van Dun, S.; Ottmann, C.; Milroy, L.-G.; Brunsveld, L. Supramolecular Chemistry Targeting Proteins. J. Am. Chem. Soc. 2017, 139, 13960-13968.
- (4) Klämer, F.-G.; Schrader, T. Aromatic Interactions by Molecular Tweezers and Clips in Chemical and Biological Systems. *Acc. Chem. Res.* **2013**, *46*, 967-978.
- (5) Reczek, J. J.; Kennedy, A. A.; Halbert, B. T.; Urbach, A. R. Multivalent Recognition of Peptides by Modular Self-Assembled Receptors. *J. Am. Chem. Soc.* **2009**, *131*, 2408-2415.
- (6) Smith, L. C.; Leach, D. G.; Blaylock, B. E.; Ali, O. A.; Urbach, A. R. Sequence-Specific, Nanomolar Peptide Binding via Cucurbit [8] uril-Induced Folding and Inclusion of Neighboring Side Chains. J. Am. Chem. Soc. 2015, 137, 3663-3669.
- (7) Sonzini, S.; Marcozzi, A.; Gubeli, R. J.; van der Walle, C. F.; Ravn, P.; Herrmann, A.; Scherman, O. A. High Affinity Recognition of a Selected Amino Acid Epitope within a Protein by Cucurbit[8]uril Complexation. *Angew. Chem. Int. Ed.* **2016**, *55*, 14000-14004.
- (8) Faggi, E.; Moure, A.; Bolte, M.; Vicent, C.; Luis, S. V.; Alfonso, I. Pseudopeptidic Cages as Receptors for N-Protected Dipeptides. *J. Org. Chem.* **2014**, *79*, 4590-4601.
- (9) Faggi, E.; Vicent, C.; Luis, S. V.; Alfonso, I. Stereoselective recognition of the Ac-Glu-Tyr-OH dipeptide by pseudopeptidic cages. *Org. Biomol. Chem.* **2015**, 13, 11721-11731.
- (10) Yapar, S.; Oikonomou, M.; Velders, A. H.; Kubik, S. Dipeptide recognition in water mediated by mixed monolayer protected gold nanoparticles. *Chem. Commun.* **2015**, *51*, 14247-14250.
- (11) Xu, Z.; Jia, S.; Wang, W.; Yuan, Z.; Jan Ravoo, B.; Guo, D.-S. Heteromultivalent peptide recognition by co-assembly of cyclodextrin and calixarene amphiphiles enables inhibition of amyloid fibrillation. *Nat. Chem.* **2019**, *11*, 86-93.
- (12) White, A. D.; Nowinski, A. K.; Huang, W. J.; Keefe, A. J.; Sun, F.; Jiang, S. Y. Decoding nonspecific interactions from nature. *Chem. Sci.* **2012**, *3*, 3488-3494.
- (13) Azevedo, C.; Saiardi, A. Why always lysine? The ongoing tale of one of the most modified amino acids. *Adv. Biol. Regul.* **2016**, *60*, 144-150.
- (14) Wang, Z. A.; Cole, P. A. The Chemical Biology of Reversible Lysine Post-translational Modifications. *Cell Chem. Biol.* **2020**, *27*, 953-969.
- (15) Zasloff, M. Antimicrobial peptides of multicellular organisms. *Nature* **2002**, 415, 389-395.
- (16) Coates, A. R.; Hu, Y. Targeting non-multiplying organisms as a way to develop novel antimicrobials. *Trends. Pharmacol. Sci.* **2008**, *29*, 143-150.
- (17) Lindgren, M.; Hällbrink, M.; Prochiantz, A.; Langel, Ü. Cell-penetrating peptides. *Trends Pharmacol. Sci.* **2000**, *21*, 99-103.
- (18) Richard, J. P.; Melikov, K.; Vives, E.; Ramos, C.; Verbeure, B.; Gait, M. J.; Chernomordik, L. V.; Lebleu, B. Cell-penetrating Peptides: A REEVALUATION OF THE MECHANISM OF CELLULAR UPTAKE. *Journal of Biological Chemistry* **2003**, 278, 585-590.
- (19) Zorko, M.; Langel, Ü. Cell-penetrating peptides: mechanism and kinetics of cargo delivery. *Adv. Drug Deliv. Rev.* **2005**, *S7*, 529-545.
- (20) Heitz, F.; Morris, M. C.; Divita, G. Twenty years of cell-penetrating peptides: from molecular mechanisms to therapeutics. *Br. J. Pharmacol.* **2009**, 157, 195-206.
- (21) Fonseca, S. B.; Pereira, M. P.; Kelley, S. O. Recent advances in the use of cell-penetrating peptides for medical and biological applications. *Adv. Drug Deliv. Rev.* **2009**, *61*, 953-964.
- (22) Zhao, Y. Sequence-Selective Recognition of Peptides in Aqueous Solution: A Supramolecular Approach through Micellar Imprinting. *Chem.-Eur. J.* **2018**, 24, 14001-14009.

- (23) Fa, S.; Zhao, Y. General Method for Peptide Recognition in Water through Bioinspired Complementarity. *Chem. Mater.* **2019**, 31, 4889-4896.
- (24) Zangiabadi, M.; Zhao, Y. Molecularly Imprinted Polymeric Receptors with Interfacial Hydrogen Bonds for Peptide Recognition in Water. ACS Appl. Polym. Mater. 2020, 2, 3171-3180.
- (25) Nishino, H.; Huang, C. S.; Shea, K. J. Selective protein capture by epitope imprinting. *Angew. Chem. Int. Ed.* **2006**, 45, 2392-2396.
- (26) Hoshino, Y.; Kodama, T.; Okahata, Y.; Shea, K. J. Peptide Imprinted Polymer Nanoparticles: A Plastic Antibody. *J. Am. Chem. Soc.* **2008**, *130*, 15242-15243.
- (27) Hoshino, Y.; Koide, H.; Urakami, T.; Kanazawa, H.; Kodama, T.; Oku, N.; Shea, K. J. Recognition, Neutralization, and Clearance of Target Peptides in the Bloodstream of Living Mice by Molecularly Imprinted Polymer Nanoparticles: A Plastic Antibody. *J. Am. Chem. Soc.* **2010**, *132*, 6644-6645.
- (28) Urraca, J. L.; Aureliano, C. S. A.; Schillinger, E.; Esselmann, H.; Wiltfang, J.; Sellergren, B. Polymeric Complements to the Alzheimer's Disease Biomarker β -Amyloid Isoforms A β 1–40 and A β 1–42 for Blood Serum Analysis under Denaturing Conditions. *J. Am. Chem. Soc.* **2011**, *133*, 9220-9223.
- (29) Banerjee, S.; König, B. Molecular Imprinting of Luminescent Vesicles. *J. Am. Chem. Soc.* **2013**, *135*, 2967-2970.
- (30) Qader, A. A.; Urraca, J.; Torsetnes, S. B.; Tønnesen, F.; Reubsaet, L.; Sellergren, B. Peptide imprinted receptors for the determination of the small cell lung cancer associated biomarker progastrin releasing peptide. *J. Chromatogr. A* **2014**, *1370*, 56-62.
- (31) Zhang, Y.; Deng, C.; Liu, S.; Wu, J.; Chen, Z.; Li, C.; Lu, W. Active Targeting of Tumors through Conformational Epitope Imprinting. *Angew. Chem. Int. Ed.* **2015**, *54*, 5157-5160.
- (32) Schwark, S.; Sun, W.; Stute, J.; Lutkemeyer, D.; Ulbricht, M.; Sellergren, B. Monoclonal antibody capture from cell culture supernatants using epitope imprinted macroporous membranes. *RSC Adv.* **2016**, *6*, 53162-53169.
- (33) Xing, R.; Ma, Y.; Wang, Y.; Wen, Y.; Liu, Z. Specific recognition of proteins and peptides via controllable oriented surface imprinting of boronate affinity-anchored epitopes. *Chem. Sci.* **2019**, *10*, 1831-1835.
- (34) Zangiabadi, M.; Ghosh, A.; Zhao, Y. Nanoparticle Scanners for the Identification of Key Sequences Involved in the Assembly and Disassembly of β -Amyloid Peptides. ACS Nano **2023**, 17, 4764-4774.
- (35) V Chowdhry, a.; Westheimer, F. H. Photoaffinity Labeling of Biological Systems. *Ann. Rev. Biochem.* **1979**, *48*, 293-325.
- (36) Leyva, E.; Young, M. J. T.; Platz, M. S. High yields of formal CH insertion products in the reactions of polyfluorinated aromatic nitrenes. *J. Am. Chem. Soc.* **1986**, *108*, 8307-8309.
- (37) Schnapp, K. A.; Platz, M. S. A laser flash photolysis study of di-, tri- and tetrafluorinated phenylnitrenes; implications for photoaffinity labeling. *Bioconjugate Chem.* **1993**, *4*, 178-183.
- (38) Schnapp, K. A.; Poe, R.; Leyva, E.; Soundararajan, N.; Platz, M. S. Exploratory photochemistry of fluorinated aryl azides. Implications for the design of photoaffinity labeling reagents. *Bioconjugate Chem.* **1993**, *4*, 172-177.
- (39) Li, X.; Palhano Zanela, T. M.; Underbakke, E. S.; Zhao, Y. Controlling Kinase Activities by Selective Inhibition of Peptide Substrates. *J. Am. Chem. Soc.* **2021**, *143*, 639-643.
- (40) Ghosh, A.; Sharma, M.; Zhao, Y. Cell-penetrating protein-recognizing polymeric nanoparticles through dynamic covalent chemistry and double imprinting. *Nat. Commun.* **2024**, *15*, 3731.

